Supporting Information

Spectral Tuning of Chlorophylls in Proteins – Electrostatics vs. Ring Deformation

Yigal Lahav[1,2], Dror Noy[2,3]* and Igor Schapiro[1]*

[1] Fritz Haber Center for Molecular Dynamics Research,

Institute of Chemistry, Hebrew University of Jerusalem, Israel.

[2] MIGAL – Galilee Research Institute, S. Industrial Zone, Kyrat Shmona, Israel.

[3] Faculty of Sciences and Technology, Tel-Hai Academic College, Upper Galilee, Israel.

Table of Contents

S1. The Effect of the Level of Theory on the Geometry Optimization

In order to examine how the level of theory used in the geometry optimization effects the spectral shift we tested different density functionals. To this end 100 equidistant snapshots were sampled from the MD production run, as described in in the computational methods section of the main text. The QM/MM relaxation step was performed with different XC functionals (PBE, BP86, BLYP and B3LYP) combined with the Def2-SVP[1,2] basis set and Grimme's dispersion correction with Becke-Johnson damping[3]. Resolution of Identity approximation (RI)[4] was used to calculate the two electron integrals. The results, shown in Table S1 and Fig. S1 suggest that the main quantity affected by the change of the XC functional is the global shift δ of the absorption maximum, which indicates the energy difference between the calculated and measured spectra. We note that the contribution of the geometry to the spectral shift increases from 22-27% in pure GGA to 38% in the hybrid functional. Inspection of the averaged geometries, obtained at the different levels of theory, result in nearly identical geometries (Fig S2). Based on the results of our benchmark the use of BLYP[5,6] functional appears to be an efficient alternative for the B3LYP[7] functional. The first 10 excitation energies for the snapshots closest to their respective of the absorption peaks are reported at tables S2-S5.

Table S1. The effect of the level of theory for geometry optimization on the spectral shift in WSCP. The spectral shift was calculated as described in the computational methods section of the main text.

Functional	Shift in protein [eV]	Shift in gas phase [eV]	δ [eV]
PBE[8]	0.019	0.005	-0.1508
BP86[5,9]	0.018	0.004	-0.1468
BLYP[5,6]	0.022	0.006	-0.1398
B3LYP[7]*	0.026	0.01	-0.1953

*The COSX approximation was used to calculate HF exchange.

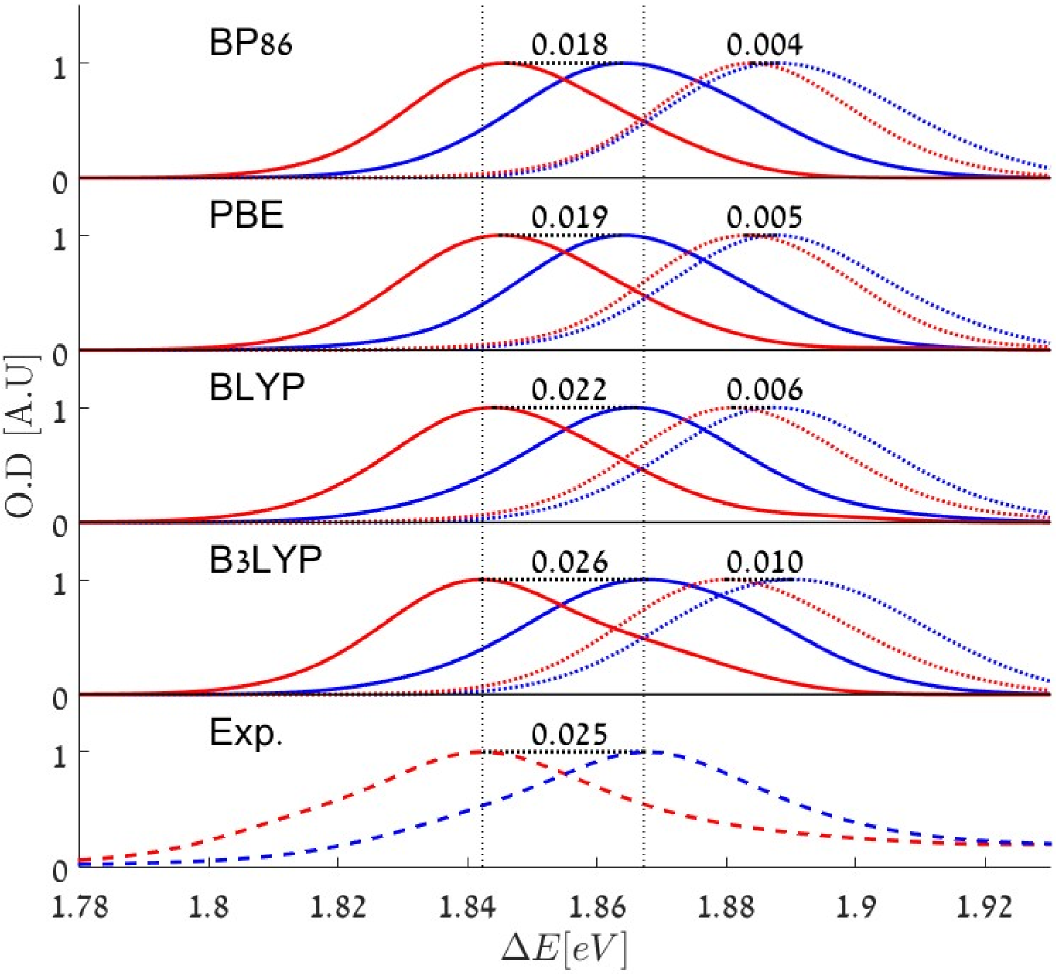

Figure S1. Absorption bands of CaWSCP (red) and LvWSCP (blue), using different ground state levels of theory in comparison to the experimental counterpart (bottom, dashed line). Excitation energies were calculated inside the protein environment (solid line) and with the protein charges set to zero (dotted lines). Results were shifted according to the δ values on Table S1.

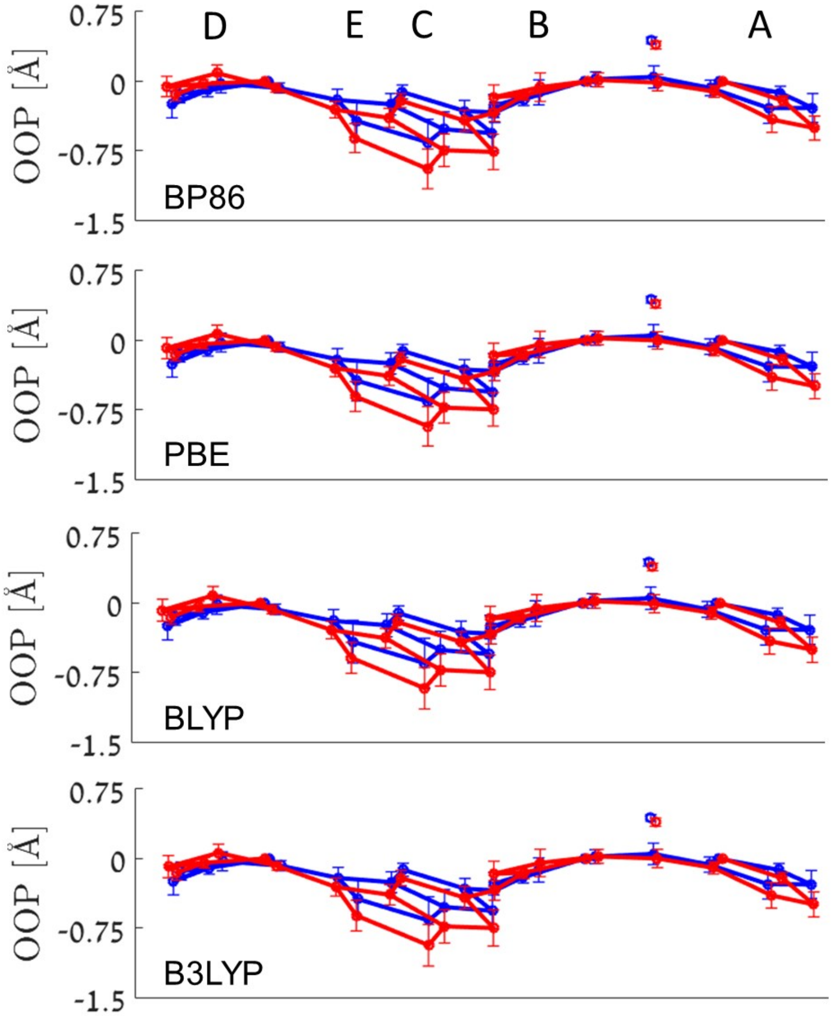

Figure S2. Out of plane displacement of the Chl macrocycle atoms in CaWSCP (red) and LvWSCP (blue), at different ground state levels of theory. Standard deviations are represented by bars.

Table S2. The first 10 excitation energies of LvWSCP and CaWSCP taken from the sample closest to the absorption maximum at the ground state level of theory **B3LYP**/def2-SVP. Excitation energies are reported in eV and shifted according to table S1.

	LvWSCP		CaWSCP	
	Excitation energy	Oscillator Strength	Excitation energy	Oscillator Strength
S_1	1.8677	0.1926	1.8419	0.2161
S_2	2.1602	0.0514	2.1129	0.0491
S_3	3.0239	0.0071	2.7903	0.0000
S_4	3.0400	0.5371	3.0718	0.0002
S_5	3.2419	0.3785	3.0798	0.7447
S_6	3.2870	0.4212	3.1427	0.0002
S_7	3.2905	0.1812	3.2886	0.7580
S_8	3.3264	0.0000	3.3126	0.0800
S_9	3.3742	0.0002	3.4898	0.0482
S_{10}	3.5594	0.0277	3.5185	0.0001

Table S3. The first 10 excitation energies of LvWSCP and CaWSCP taken from the sample closest to the absorption maximum at the ground state level of theory **BLYP**/def2-SVP. Excitation energies are reported in eV and shifted according to table S1.

	LvWSCP		CaWSCP	
	Excitation energy	Oscillator Strength	Excitation energy	Oscillator Strength
S_1	1.8656	0.2004	1.8439	0.2398
S_2	2.1411	0.0526	2.1150	0.0580
S_3	2.9783	0.0000	2.6602	0.0001
S_4	3.0818	0.5787	2.9263	0.0003
S_5	3.2440	0.2298	3.0010	0.0001
S_6	3.2604	0.0000	3.0914	0.7049
S_7	3.3171	0.7355	3.2432	0.4483
S_8	3.5454	0.0418	3.3169	0.4674
S_9	3.5895	0.0002	3.4045	0.0002
S_{10}	3.6300	0.0000	3.4551	0.0193

Table S4. The first 10 excitation energies of LvWSCP and CaWSCP taken from the sample closest to the absorption maximum at the ground state level of theory **PBE**/def2-SVP. Excitation energies are reported in eV and shifted according to table S1.

	LvWSCP		CaWSCP	
	Excitation energy	Oscillator Strength	Excitation energy	Oscillator Strength
S_1	1.8643	0.1907	1.8452	0.2398
S_2	2.1388	0.0411	2.0590	0.0000
S_3	2.9033	0.0000	2.1227	0.0426
S_4	3.0458	0.6037	2.3613	0.0000
S_5	3.1865	0.0001	2.6796	0.0001
S_6	3.2437	0.0000	3.0981	0.6261
S_7	3.2573	0.2409	3.1994	0.3037
S_8	3.2896	0.7292	3.3234	0.7177
S_9	3.3602	0.0083	3.3382	0.0000
S_{10}	3.5728	0.0532	3.3776	0.0000

Table S5. The first 10 excitation energies of LvWSCP and CaWSCP taken from the sample closest to the absorption maximum at the ground state level of theory **BP86**/def2-SVP. Excitation energies are reported in eV and shifted according to table S1.

	LvWSCP		CaWSCP	
	Excitation energy	Oscillator Strength	Excitation energy	Oscillator Strength
S_1	1.8644	0.1924	1.8452	0.2246
S_2	2.1252	0.0380	2.1109	0.0410
S_3	2.9498	0.0004	2.4605	0.0000
S_4	3.0555	0.6925	2.7647	0.0000
S_5	3.2129	0.0010	3.0897	0.6842
S_6	3.2660	0.8154	3.1279	0.0003
S_7	3.3111	0.0000	3.2544	0.2658
S_8	3.3915	0.0508	3.3184	0.6826
S_9	3.4134	0.0067	3.5314	0.0250
S_{10}	3.4407	0.0000	3.5863	0.0034

S2. Spectral Tuning Mechanism in a Pont Charge Model

To rationalize the effect of electrostatics on the Chl absorption spectra, we performed the following test: one point charge (c_1) was placed 1*nm* away from ring A, and additional one (c_2) 1*nm* from ring B. These point charges are mimicking the changes in the electrostatic potential between the two types of WSCP as illustrated in Fig. 6 of the main text. The value of point charges was varied between −1 and 1 in steps of 0.2*e*, and excitation energy was calculated at the CAM-B3LYP/Def2-SVP level of theory (Fig. S3). This simple test confirms our rationale that a positive electrostatic potential on ring A leads to a red shift of the Chl excitation energy, due to the excess of electron density on that ring in the excited state. In a similar fashion negative potential results in a blue shift. A positive potential applied on ring B leads to blue shift, due to the excess of electron density on that ring in the ground state (Fig. 5 in the main text). A negative point charge, close to ring B, results in a red shift.

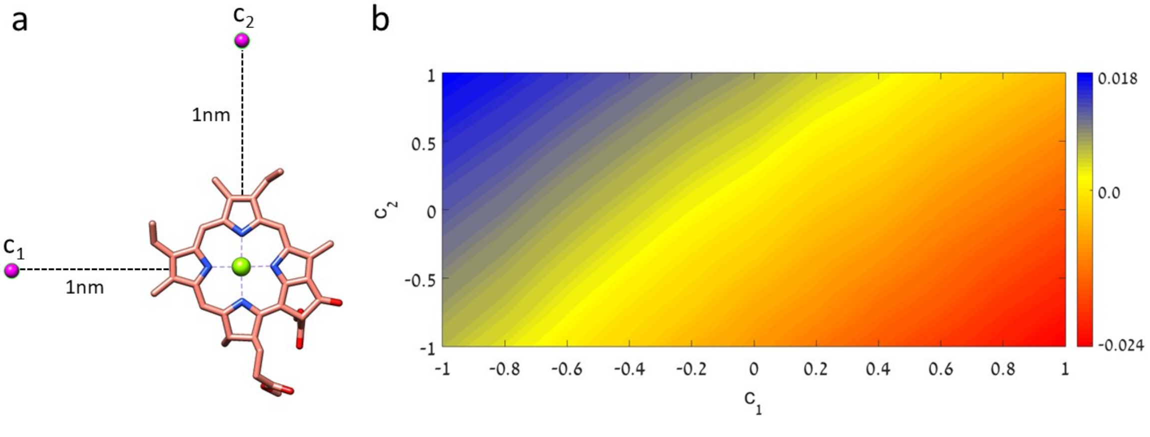

Figure S3. The effect of point charge on the Chl excitation energy. (a) Chl with two point charges c_1 and c_2 located 1nm from rings A and B respectively. (b) Spectral shift in eV with respect to charge values c_1 and c_2.

S3. Analysis of the Experimental Electron Density and Structure

The QM/MM geometry obtained for the Chl in LvWSCP was found to be in poor agreement with the geometry described in the crystal structure. Thus, required further investigation. By visualizing the electron density that was obtained experimentally[10,11] and used to fit the structures of CaWSCP and LvWSCP (Fig. S4), it is clear that for both WSCP types the Chl macrocycles are not planar, and that the planar conformation assigned to the Chl in LvWSCP is not the best fit to the electron density. Indeed, a version with a better fitted more bent Chl conformation is available from the PDB REDO database[12]. Quantitative comparison, based on the Chl macrocycle out-of-plane displacement, was performed between the three different Chl structures: The original PDB of LvWSCP (2DRE), its refined version from the PDB REDO database[12], and the QM/MM averaged geometry of LvWSCP (Fig. S5). The comparison showed that the geometry taken from the REDO database is in good agreement with the QM/MM simulation, especially in the region of the A ring. Based on the electron densities (Fig. S4) and the out-of-plane deviation analysis (Fig. S5), it appears that the LvWSCP chlorophyll geometry as presented in the original PDB structure is poorly fitted.

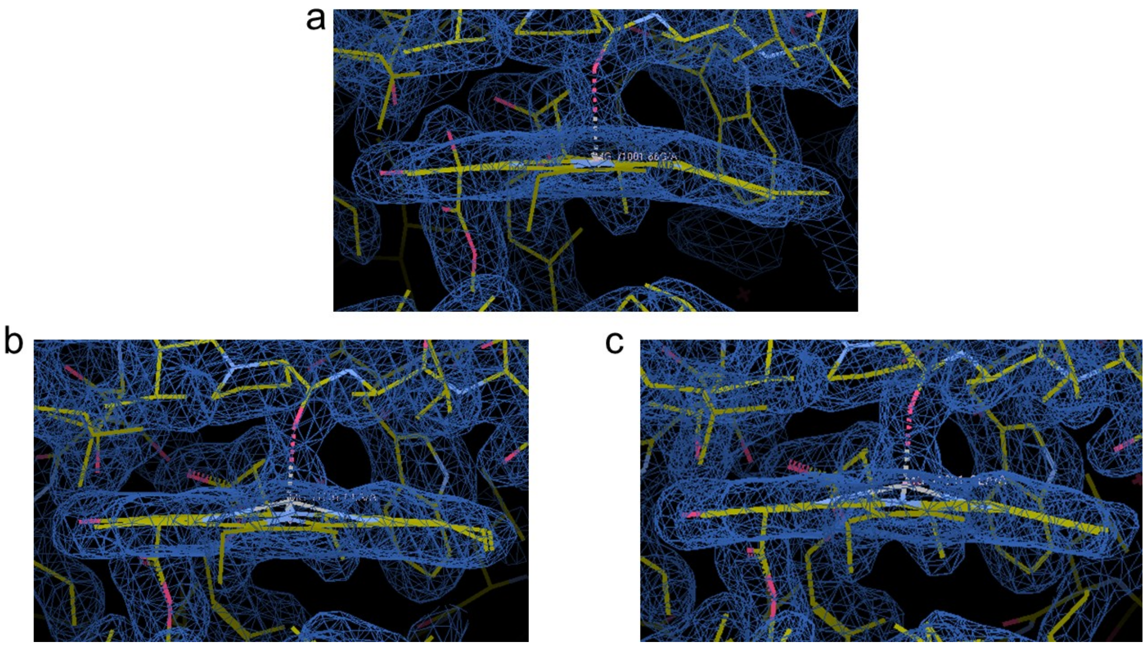

Figure S4. Measured electron density and fitted molecular structures (line representation) of CaWSCP (a), LvWSCP (b), and LvWSCP from the REDO database (c). Visualization was done using the Coot program.[25]

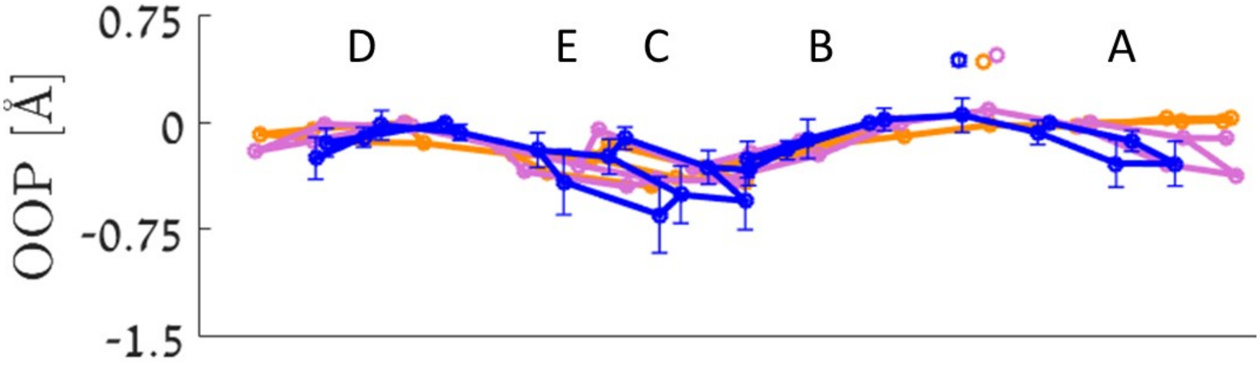

Figure S5. Out of plane (OOP) displacement of different LvWSCP structures: original PDB (orange), PDB REDO database (purple), QM/MM averaged geometry (blue).

References

1 T. Yanai, D. P. Tew and N. C. Handy, *Chem. Phys. Lett.*, 2004, **393**, 51–57.

2 W. Florian and A. Reinhart, *Phys. Chem. Chem. Phys.*, 2005, **7**, 3297–3305.

3 S. Grimme, S. Ehrlich and L. Goerigk, *J. Comput. Chem.*, 2011, **32**, 1456–1465.

4 O. Vahtras, J. Almlöf and M. W. Feyereisen, *Chem. Phys. Lett.*, 1993, **213**, 514–518.

5 A. D. Becke, *Phys. Rev. A*, 1988, **38**, 3098–3100.

6 C. Lee, W. Yang and R. G. Parr, *Phys. Rev. B*, 1988, **37**, 785–789.

7 A. D. Becke, *J. Chem. Phys.*, 1993, **98**, 5648–5652.

8 J. P. Perdew, K. Burke and M. Ernzerhof, 1996, 3865–3868.

9 J. P. Perdew, *Phys. Rev. B*, 1986, **33**, 8822–8824.

10 B. Dominika, D. Orly, P. Vadivel, P. Yoav, P. D. H. and N. Dror, *Angew. Chemie Int. Ed.*, **55**, 6901–6905.

11 I. Oonishi, H. Satoh, A. Nakagawa, N. Itoh, A. Uchida, K. Mitsunaga and D. Horigome, *J. Biol. Chem.*, 2006, **282**, 6525–6531.

12 R. P. Joosten, T. A. H. te Beek, E. Krieger, M. L. Hekkelman, R. W. W. Hooft, R. Schneider, C. Sander and G. Vriend, *Nucleic Acids Res.*, 2010, **39**, D411--D419.